FTIR Spectroscopy of *Synechocystis* 6803 Mutants Affected on the Hydrogen Bonds to the Carbonyl Groups of the PsaA Chlorophyll of P700 Supports an Extensive Delocalization of the Charge in $P700^{+}$†

Maria Pantelidou,‡ Parag R. Chitnis,‡ and Jacques Breton*,§

Department of Biochemistry, Biophysics, and Molecular Biology, Iowa State University, Ames, Iowa 50011, and Service de Bioénergétique, CEA-Saclay, 91191 Gif-sur-Yvette, France

Received March 11, 2004; Revised Manuscript Received May 3, 2004

ABSTRACT: P700, the primary electron donor of photosystem I is an asymmetric dimer made of one molecule of chlorophyll *a*′ (P_A) and one of chlorophyll *a* (P_B). While the carbonyl groups of P_A are involved in hydrogen-bonding interactions with several surrounding amino acid side chains and a water molecule, P_B does not engage in hydrogen bonding with the protein. Light-induced FTIR difference spectroscopy of the photooxidation of P700 has been combined with site-directed mutagenesis in *Synechocystis* sp. PCC 6803 to investigate the influence of these hydrogen bonds on the structure of P700 and $P700^{+}$. When the residue Thr A739, which donates a hydrogen bond to the 9-keto C═O group of P_A, is changed to Phe, a differential signal at 1653(+)/1638(−) cm^{-1} in the $P700^{+}$/P700 FTIR difference spectrum upshifts by ∼30−40 cm^{-1}, as expected for the rupture of the hydrogen bond or, at least, a strong decrease of its strength. The same upshift is also observed in the FTIR spectrum of a triple mutant in which the residues involved in the three main hydrogen bonds to the 9-keto and 10a-carbomethoxy groups of P_A have been changed to the symmetry-related side chains present around P_B. In addition, the spectrum of the triple mutant shows a decrease of a differential signal around 1735 cm^{-1} and the appearance of a new signal around 1760 cm^{-1}. This is consistent with the perturbation of a bound 10a-ester C═O group that becomes free in the triple mutant. All of these observations support the assignment scheme proposed previously for the carbonyls of P700 and $P700^{+}$ [Breton, J., Nabedryk, E., and Leibl, W. (1999) *Biochemistry 38*, 11585−11592] and therefore reinforce our previous conclusions that the positive charge in $P700^{+}$ is largely delocalized over P_A and P_B.

The reaction center (RC)[1] of photosystem I (PS I) is a large multisubunit integral membrane protein that uses light to drive electrons across the photosynthetic membrane of cyanobacteria, algae, and plants. Most of the cofactors involved in light collection and electron-transfer processes are coordinated to the two main subunits, PsaA and PsaB, each containing 11 transmembrane α helices that form the heterodimeric core of the RC. Light absorbed by an antenna pigment is rapidly trapped by a specialized dimer of excitonically coupled chlorophyll (Chl) molecules called P700, which is the primary electron donor of PS I. After excitation, an electron is ejected from the lowest excited state of P700 and is first passed onto a monomeric Chl. Subsequent charge stabilization is achieved by further electron-transfer steps over a chain of acceptors. Owing to its prominent role, the structure of P700 in its neutral, triplet, and cationic states has been investigated in great detail using optical, vibrational, and magnetic resonance spectroscopic techniques leading to models for the organization of the pigments within the dimer and the distribution of charge and spin in the oxidized and triplet states of P700 (reviewed in ref *1*).

In the last two decades, X-ray crystallographic models of bacterial RC proteins have provided an invaluable source of information to complement the data obtained on their primary electron donors (P) by spectroscopy alone, notably when the resolution of the structures becomes sufficient to identify the amino acid side chains interacting with the pigments through hydrogen bonds to the carbonyl groups or axial ligation to the central Mg atoms of the bacteriochlorophyll (BChl) molecules. In this case, site-directed mutagenesis becomes a choice method to perturb selectively the pigment−protein interactions, therefore providing RCs with modified P, the structure and function of which can be probed by spectroscopy (reviewed in ref *2*). While X-ray crystallography provides key information on the geometry of the amino acid side chains acting as axial ligands or hydrogen-bond partners of the BChls in the ground state of P, it remains silent on several important aspects of the electronic structure of the special pair after charge separation occurs, such as the localization of the triplet state in ^3P or the hydrogen-bonding status of the BChls and the charge distribution in

† Part of this work was supported by NSF Grant MCB 0078268 to P.R.C.

* To whom correspondence should be addressed: Service de Bioénergétique, Bât. 532, CEA-Saclay, 91191 Gif-sur-Yvette Cedex, France. Telephone: (331) 6908 2239. Fax: (331) 6908 8717. E-mail: cadara3@dsvidf.cea.fr.

‡ Iowa State University.

§ CEA-Saclay.

[1] Abbreviations: (B)Chl, (bacterio)chlorophyll; PS I, photosystem I; RC, reaction center; P, primary electron donor; FTIR, Fourier transform infrared; hfc, hyperfine coupling constant; *Synechocystis*, *Synechocystis* sp. PCC 6803.

10.1021/bi049515j CCC: $27.50
Published on Web 06/08/2004

P^+. Among the spectroscopic tools that can bring specific information on the structure−function relationship in both native and genetically modified RCs, light-induced FTIR difference spectroscopy has emerged as a prominent technique (reviewed in refs *3*−*6*). The complementary aspects of the spectroscopic and X-ray crystallographic approaches have been initially encountered in the field of purple photosynthetic bacteria. This combined approach is now striding along for the PS I and is also making progress in the case of PS II.

In the case of PS I, an initial structure at 4 Å resolution (*7*) showed P700 to be a dimer of Chl with a geometry similar to that of P in the RC of photosynthetic purple bacteria, where His residues from the two homologous L and M polypeptides making up the core of the RC act as ligands to the Mg atom of the two BChl molecules of P. This observation led to an investigation of the $P700^+$/P700 FTIR difference spectra characterizing the photooxidation of P700 in a series of PS I mutants of *Chlamydomonas reinhardtii*, in which each of the conserved pairs of His located symmetrically on the homologous PsaA and PsaB polypeptides is replaced by Gln. This study allowed an identification of the His axial ligand of each of the PsaA and PsaB Chl molecules of P700 (*8*). In the following, these Chls will be termed P_A and P_B in the ground state and P_A^+ and P_B^+ in the oxidized state. In a study of P700 photooxidation in the cyanobacterium *Synechocystis* sp. PCC 6803 (referred to in the following as *Synechocystis*) that combined global isotope labeling and a comparison of $P700^+$/P700 and ^{3}P700/P700 FTIR difference spectra, it was possible for the first time to assign the 9-keto and 10a-ester C═O modes of the two Chls in P700 and $P700^+$ (*9*). Notably, it was concluded that both carbonyl groups of one Chl are free from interactions with the protein, while the two carbonyl groups of the other Chl are engaged in hydrogen-bonding interactions. An extreme downshift of 60 cm^{-1} was observed for the 9-keto C═O group of the latter Chl. The asymmetry in hydrogen bonding of the P700 Chls was found to remain in the $P700^+$ state, and upon assuming a comparable extinction coefficient for the carbonyl groups of the two Chls, it was concluded that the positive charge in $P700^+$ is approximately equally shared between the two Chls. On the other hand, the triplet state in ^{3}P700 was observed to be fully localized on the Chl that is engaged in strong bonding interactions with the protein.

When the first X-ray model of PS I from the cyanobacterium *Synechococcus elongatus* with a resolution (2.5 Å) sufficient to analyze the protein−cofactor interactions was reported (*10*), it became clear that P700 is indeed a very asymmetrical dimer (Figure 1). While P_B is a Chl *a* molecule with no hydrogen bond to the nearby PsaB polypeptide, P_A is a Chl *a*′ (epimer of Chl *a* at C_{10}) with both the 9-keto C═O and 10a-carbomethoxy groups forming hydrogen bonds with the PsaA polypeptide, either directly or through an intervening water molecule. An additional hydrogen bond between the PsaA polypeptide and the 7c-ester C═O of P_A was also described with no symmetrical interaction on the PsaB side. It should be stressed that the 7c-ester C═O group being out of conjugation to the Chl macrocycle is therefore not expected to contribute directly to a $P700^+$/P700 FTIR difference spectrum (*11*). Finally, the His residues axial ligands of the two Chl molecules of P700 observed by X-ray

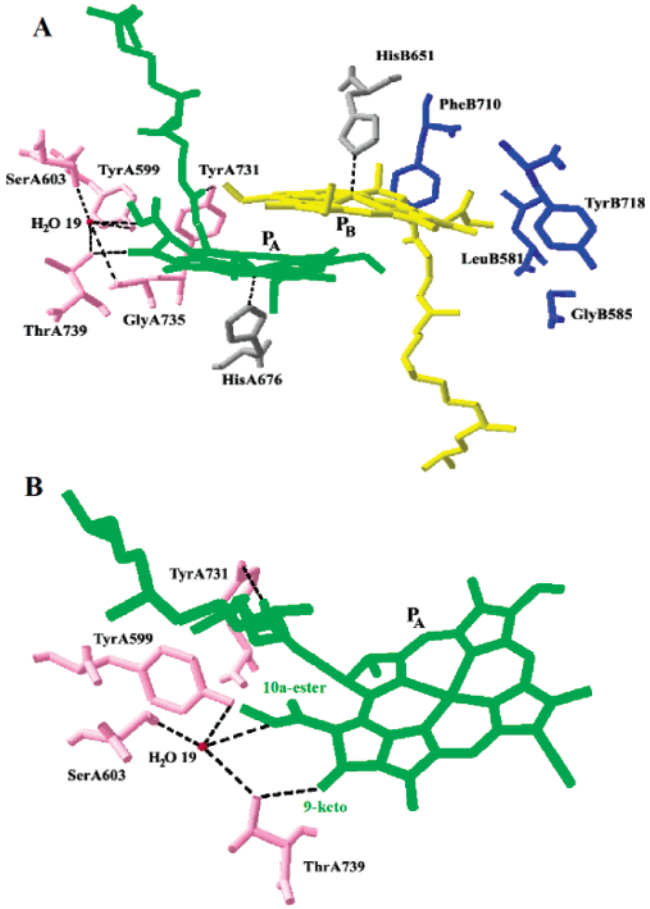

FIGURE 1: Structural model of P700, the primary electron donor of photosystem I. (A) General view along the pseudo-C_2 symmetry axis showing the organization of the dimer of Chl *a* (P_B) and Chl *a*′ (P_A) with their central Mg atoms coordinated to the side chains of His B651 and His A676, respectively. Also shown are the amino acid residues located in the close vicinity of water H_2O-19 and of the carbonyl groups of P700. Note the residues engaged in putative hydrogen bonds with the carbonyls of P_A and the symmetry-related side chains that appear free from hydrogen-bonding interactions with P_B. (B) A different view of the region surrounding the 9-keto and 10a-ester carbonyls of P_A.

crystallography turned out to be those assigned from the FTIR spectra (*8*).

Thus, the predictions from the FTIR studies (*8*, *9*) turned out to be in excellent agreement with the newest X-ray model (*6*, *10*). On the other hand, the conclusion on the delocalization of the positive charge in $P700^+$ was at variance with the interpretation of a number of previous investigations using magnetic resonance techniques, notably some recent ENDOR studies on oriented PS I crystals and on *C. reinhardtii* bearing mutations on the His axial ligands to the P700 Chls, which had led to the conclusion that the spin in $P700^+$ is essentially localized (≥85%) on P_B^+ (*1*, *12*). A further discrepancy with the results from magnetic resonance spectroscopy was noticed for the localization of the triplet character in ^{3}P700, which, at that time, was proposed to be on P_B from ADMR experiments (*1*, *13*, *14*) and on P_A from the FTIR study (*6*, *9*). The strong divergence between the conclusions derived from magnetic resonance spectroscopy and the FTIR experiments led Hastings et al. (*15*) to propose an alternative interpretation of the FTIR difference spectra with a completely different assignment for the 9-keto C═O of the P_A Chl, but that was more consistent with the

Table 1: Hydrogen-Bonding Residues of PsaA (and Homologues in PsaB) in *S. elongatus* and *Synechocystis* sp. PCC6803[a]

S. elongatus		*Synechocystis* sp.	
Tyr A603	Leu B590	Tyr A599	Leu B581
Ser A607	Gly B594	Ser A603	Gly B585
Thr A743	Tyr B727	Thr A739	Tyr B718

[a] On the basis of the 2.5-Å crystal structure of PS I in *S. elongatus* by Jordan et al. (*10*).

interpretation of the magnetic resonance experiments. The later set of assignments were critically discussed in a subsequent investigation by FTIR spectroscopy of *Synechocystis* PS I preparations bearing mutations at the His axial ligand of the PsaB Chl (*16*). It was further shown in the latter study that the imidazole C_5-N_τ stretching mode of each of the two His axial ligands of the P700 Chls were similarly perturbed upon $P700^+$ formation, an observation supporting the proposal of extensive charge delocalization derived from our previous FTIR studies (*6*, *9*).

The 2.5 Å resolution model of P700 shows a complex array of hydrogen bonds in the vicinity of the 9-keto and 10a-ester C═O groups of P_A that also involves the water molecule H_2O-19 and several of the PsaA side chains. Notably, the amino acid residue Thr A743 (the equivalent residue is Thr A739 in both *Synechocystis* and *C. reinhardtii*; see Table 1 for the correspondence with the *S. elongatus* numbering) is within hydrogen-bonding distance to both the 9-keto C═O of P_A and the H_2O-19 molecule (Figure 1, with numbering according to the sequence of *Synechocystis*). The X-ray model shows that the oxygen atom of H_2O-19, which is 3.2 Å away from the methoxy oxygen atom of the 10a-ester carbomethoxy group, is also within hydrogen-bonding distance of Tyr A603 (2.7 Å), Ser A607 (2.9 Å), and to a lesser extent, Gly A739 (3.3 Å). All of these amino acid residues are highly conserved in *Synechocystis* and are numbered Tyr A599, Ser A603, and Gly A735, respectively (Table 1). On the basis of the X-ray structural model, several mutations at the residue Thr A739 were generated in *C. reinhardtii* and their effects were investigated with structural spectroscopy techniques (*14*, *17*). Although an initial report of the results of optical and magnetic resonance spectroscopy was presented, confirming the previous conclusions that the spin in $P700^+$ and the triplet character in $^3P700$ were essentially localized on P_B (*14*), a later study that included FTIR difference spectroscopy of P700 photooxidation led to a substantial change of opinion (*17*). It was notably proposed that the interpretation of previous optical measurements of P700 photooxidation was based on invalid assumptions concerning the coupling among the pigments. As a consequence, the conclusions from the ADMR measurements on the localization on P_B of the triplet in $^3P700$ had to be revised. Similarly, the ENDOR measurements on the new mutants indicated that the extent of electronic coupling among the two Chls in $P700^+$ of the wild type was larger than previously thought. On the other hand, the FTIR results on the mutants were taken to show the alteration of the hydrogen bond to the 9-keto carbonyl of P_A in the mutants. Although the absence of FTIR studies of isotopically labeled samples or of the triplet state of the mutants precluded a firm and direct assignment of the bands in the mutants, the FTIR data of Witt et al. (*17*) could be easily interpreted in the frame of the model previously put forward for the assignment of the carbonyl bands in P700, $P700^+$, and $^3P700$ (*6*, *9*). In contrast, a detailed FTIR study of another *C. reinhardtii* mutant at Thr A739 has been recently presented (*18*) as supporting the assignment scheme of Hastings et al. (*15*) for the 9-keto C═O group of P_A.

In the present study, we report on the $P700^+$/P700 FTIR difference spectrum of PS I trimers from *Synechocystis* in which the residue Thr A739 in hydrogen-bonding interaction with the 9-keto C═O of P_A has been replaced with the non-hydrogen-bonding Phe side chain. The FTIR spectrum of this single mutant is compared to that of PS I bearing a set of three mutations that were devised to alter the hydrogen-bonding pattern of the 9-keto and 10a-carbomethoxy groups of the PsaA Chl of P700 by making it similar to the environment of the symmetry-related PsaB Chl that exhibits no hydrogen-bonding interaction with the protein (Figure 1).

MATERIALS AND METHODS

Site-Directed Mutagenesis. Site-specific mutations in *psaA* gene were performed with pIBC as the donor plasmid and pWX as the recipient *Synechocystis* strain, as described in ref *19*. Strain pWX lacks a part of *psaA* and the whole *psaB* gene. Plasmid pIBC consists mostly of *psaA* gene, *psaB* gene, and its 760-bp downstream region incorporated into the pBluescript II KS vector. A chloramphenicol resistance cassette gene is located after the 3′ terminator of the *psaB* gene. PCR mutagenesis was performed using the *Platinum Pfx Polymerase* (Invitrogen) and pIBC as a template. The mutation containing DNA was selected by digestion with *Dpn*I endonuclease (Promega). The mutated plasmids were checked by sequencing and were used to transform the recipient strain, pWX. The transformants were selected and segregated for several generations on chloramphenicol-supplemented BG-11 plates under low-light intensity (2−3 μmol m^{-2} s^{-1}) at 30 °C. The fragment containing the site-specific mutations was amplified from genomic DNA by PCR and was sequenced to confirm the presence of the desired mutations. In the single mutant, the Thr PsaA 739 (Thr A739) is replaced by Phe, while in the triple mutant, Tyr A599, Ser A603, and Thr A739 are mutated to Leu, Gly, and Tyr, respectively.

Cell Growth and PS I Complex Isolation. The *Synechocystis* wild-type and mutant strains were grown in BG-11 medium at 30 °C. The cultures were grown in large bottles with aeration, under light intensity of 40−50 μmol photons m^{-2} s^{-1}. The mutants were supplemented with 30 mg/L chloramphenicol, and all strains were grown in the presence of glucose (5 mM). For global ^{15}N labeling of cells, the cultures were grown in ^{15}N-labeled media. BG-11 was supplemented with $Na^{15}NO_3$ (from $H^{15}NO_3$ purchased from Cambridge Isotope Laboratories). Growth was monitored by absorbance measurements at 730 nm (A_{730}) with a UV-160U spectrophotometer (Shimadzu). The cells were harvested at mid to late exponential growth (1.0 OD_{730}) with centrifugation at 4000*g*. Thylakoid membrane extraction and isolation of PS I trimers was performed according to previously published methods with minor alterations (*20*). PS I complexes were concentrated to 1 mg of Chl/mL and stored at −60 °C.

FTIR Measurements. Samples for FTIR were prepared by centrifugation (300 000*g* for 60 min) of PS I trimers in Tris-

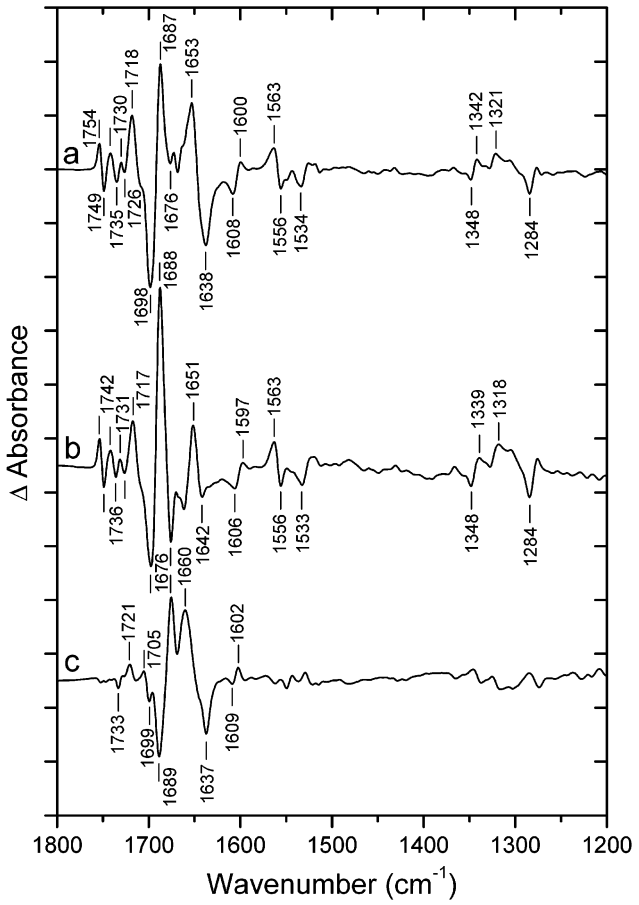

FIGURE 2: Light-induced $P700^+/P700$ FTIR difference spectrum of PS I complexes from *Synechocystis* sp. PCC 6803 at 5 °C. (a) Wild-type PS I and (b) mutant T(A739)F. (c) Double-difference spectrum of the wild-type minus T(A739)F mutant. Each division on the vertical scale corresponds to 5×10^{-4} absorbance unit. About 100 000 interferograms were added. The frequency of the bands is given as ± 1 cm^{-1}.

HCl buffer (70 mM at pH 7.0) containing 80 mM potassium ferrocyanide and 20 mM potassium ferricyanide. A small fraction of the resultant pellet was squeezed between two calcium fluoride windows, and the thickness of the sample was adjusted to give an absorption of about 0.8 OD unit at the maximum around 1650 cm^{-1}, with approximately half of this absorption being due to the amide I absorption and the other half, to the scissoring mode of water. Light-induced difference spectra were recorded on Nicolet 60SX and 860 FTIR spectrometers at a temperature of 5 °C and at a resolution of 4 cm^{-1} as previously reported (*9*, *16*).

RESULTS

$P700^+/P700$ FTIR Spectrum of the T(A739)F Single Mutant. Figure 2 shows a comparison of the light-induced $P700^+/P700$ FTIR difference spectra of a wild-type control (a) and of the T(A739)F mutant (b). The two spectra have been normalized by minimizing the residuals over the whole frequency range between 1000 and 5000 cm^{-1} (not shown). The wild-type minus mutant double-difference spectrum is shown in Figure 2c. The largest impact of the mutation on the $P700^+/P700$ FTIR spectrum occurs in the spectral range characteristic of the 9-keto C═O of the Chls of P700 and $P700^+$ between 1720 and 1635 cm^{-1}. The 1653(+)/1638(−) cm^{-1} differential signal in the spectrum of the wild type (Figure 2a) is replaced by another one of greatly reduced amplitude and mostly positive at 1651(+)/1642(−) cm^{-1} in the spectrum of the mutant (Figure 2b). This is accompanied by the development of a large negative band at 1676 cm^{-1} and a positive one at 1688 cm^{-1} in the mutant that overlaps with a preexisting positive band at 1687 cm^{-1} in the wild type. Together these changes contribute the two large differential signals of comparable amplitudes but of opposite signs at 1689(−)/1676(+) and 1660(+)/1637(−) cm^{-1} in the double-difference spectrum (Figure 2c). The amplitude of the 1718/1698 cm^{-1} signal in the spectrum of the control is reduced by 15−20% in the mutant.

Above 1725 cm^{-1}, very little difference is observed between the spectrum of the wild type (Figure 2a) and that of the T(A739)F single mutant (Figure 2b), except for a ∼1 cm^{-1} upshift upon mutation of the small differential signal at 1735(−)/1730(+) cm^{-1}. This upshift is responsible for the small negative band at 1733 cm^{-1} in the double-difference spectrum (Figure 2c). On the other hand, a 2−3 cm^{-1} downshift of the macrocycle C═C marker mode of 5-coordinated Chl at 1608 cm^{-1} (*21*) is among the other significant perturbations that can be identified upon comparing the $P700^+/P700$ FTIR spectra of the wild type and the T(A739)F mutant. Similarly, the coupled C−C, C−H, and C−N modes of the Chl macrocycle absorbing between 1400 and 1250 cm^{-1} are also affected both in amplitude and in frequency by the mutation.

$P700^+/P700$ FTIR Spectrum of the Triple Mutant. Figure 3 shows a comparison of the light-induced $P700^+/P700$ FTIR difference spectra of the wild-type control (a) and of the triple mutant (b) together with the corresponding double-difference spectrum wild-type minus triple mutant (c). In the frequency range below 1725 cm^{-1} of the $P700^+/P700$ FTIR spectra, most of the changes, which are induced by the triple mutation (Figure 3b), were also observed in the spectrum of the T(A739)F single mutant (Figure 2b). The double-difference spectrum (Figure 3c), which is also very comparable to that calculated for the single mutant (Figure 2c), exhibits two large differential signals of nearly equal amplitudes but of opposite signs at 1690(−)/1676(+) and 1657(+)/1637(−) cm^{-1}. Furthermore, the spectrum of the triple mutant (Figure 3b) also exhibits a downshift of the macrocycle C═C marker mode of 5-coordinated Chl at 1608 cm^{-1} and a perturbation of the coupled C−C, C−H, and C−N modes of the Chl macrocycle in the 1400−1250 cm^{-1} frequency range as previously observed for the T(A739)F single mutant (Figure 2b). The amplitude of the 1718/1698 cm^{-1} signal in the spectrum of the control is also reduced by 15−20% in the triple mutant.

In the triple mutant, a significant alteration of the $P700^+/P700$ FTIR spectrum is detected in the frequency range typical of the 10a-ester C═O above 1725 cm^{-1}. Upon mutation, a new positive band appears at 1762 cm^{-1}, while the amplitude of the small differential signal at 1735(−)/1730(+) cm^{-1} is strongly decreased (Figure 3b). The 1742(+)/1735(−) cm^{-1} differential signal of the wild type is reduced in amplitude in the mutant spectrum. On the other hand, the differential signal at 1754(+)/1749(−) cm^{-1}, previously assigned to the free 10a-ester C═O of P_B^+/P_B (*9*), is not affected by the mutation.

Effect of Global ^{15}N Labeling on the $P700^+/P700$ FTIR Spectrum of the Triple Mutant. The 1651(+)/1642(−) cm^{-1}

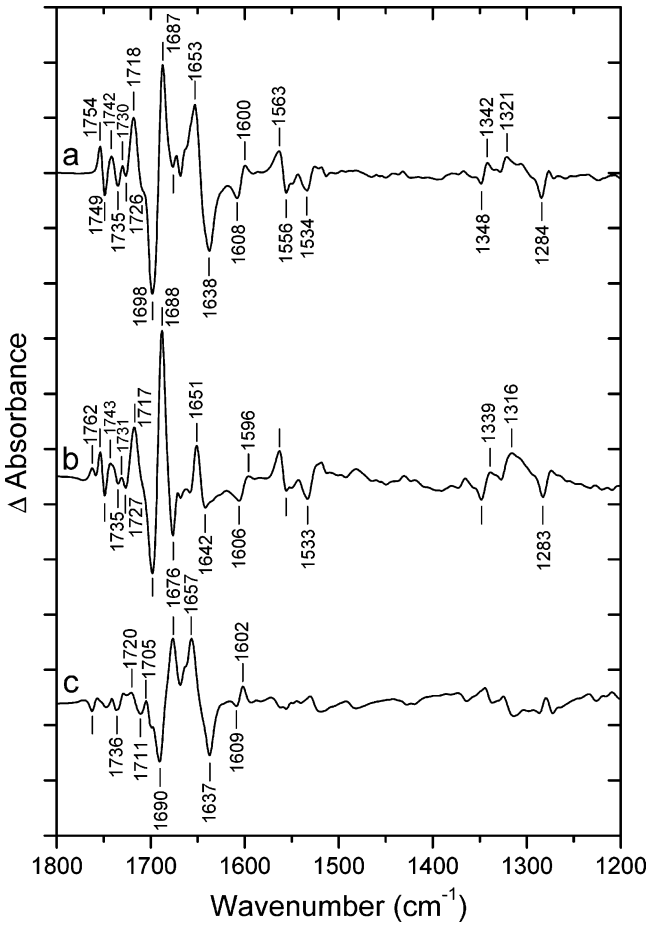

FIGURE 3: Light-induced $P700^+/P700$ FTIR difference spectrum of PS I complexes from *Synechocystis* at 5 °C. (a) Wild-type PS I and (b) a triple mutant containing the T(A739)Y, S(A603)G, and Y(A599)L changes. (c) Double-difference spectrum of the wild-type minus triple mutant. Each division on the vertical scale corresponds to 5×10^{-4} absorbance unit.

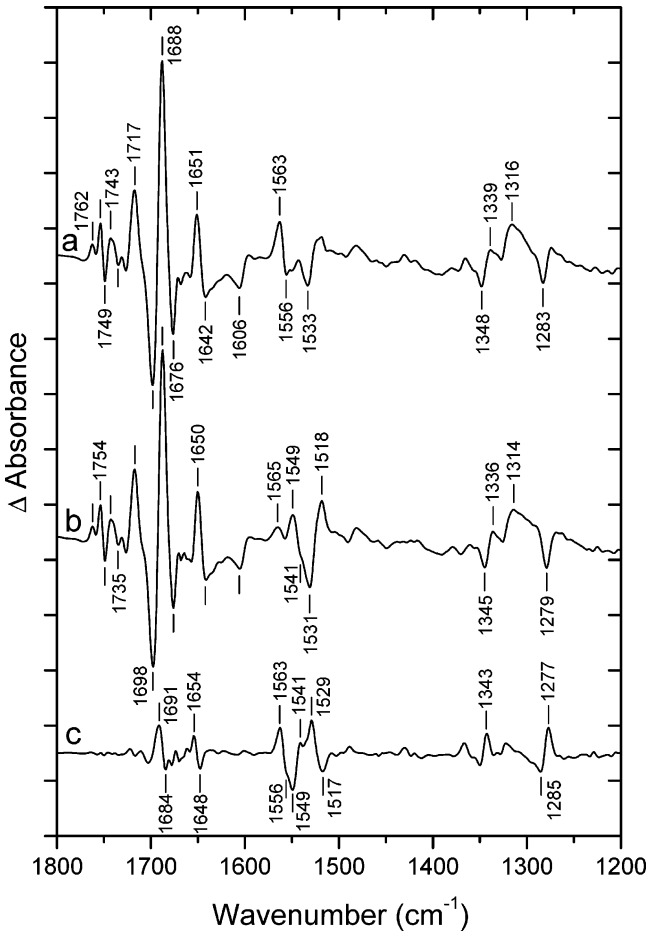

FIGURE 4: Light-induced $P700^+/P700$ FTIR difference spectrum of PS I complexes from the triple mutant *Synechocystis* at 5 °C. (a) Unlabeled PS I and (b) ^{15}N-labeled PS I. (c) Double-difference spectrum of the unlabeled minus ^{15}N-labeled. Each division on the vertical scale corresponds to 4×10^{-4} absorbance unit.

signal that remains in the spectrum of the single and triple mutants (Figures 2b and 3b) could originate from protein amide I C═O modes or from the 9-keto C═O vibration of a subpopulation of P700 Chl in hydrogen-bonding interaction with the OH group of a water molecule (or of the Tyr introduced at the PsaA 739 site in the triple mutant). To help discriminate between these two possibilities, global ^{15}N labeling was performed on the triple mutant. In Figure 4, the $P700^+/P700$ FTIR spectrum of the unlabeled sample of the triple mutant (Figure 4a) is compared to that of the uniformly ^{15}N-labeled sample (Figure 4b) and to the unlabeled minus ^{15}N-labeled double-difference spectrum (Figure 4c). The bands around 1550 cm^{-1} in the spectral range characteristic of the combined C−N stretching (40%) and N−H bending (60%) vibrations of the amide II mode are strongly affected. Notably, a differential signal at 1563(+)/1556(−) cm^{-1} exhibits upon labeling the same 14−15 cm^{-1} downshift characteristic of the amide II mode that is observed for this band in the absorption spectrum of the labeled sample (not shown). Similar changes have been previously reported for the $P700^+/P700$ FTIR spectrum of uniformly ^{15}N-labeled wild-type samples (*9*, *16*). The coupled C−C, C−H, and C−N modes of the Chl macrocycle absorbing between 1400 and 1250 cm^{-1} are also affected by the labeling. Very clear downshifts of many bands are also observed in the frequency range of the amide A band around 3300 cm^{-1}, corresponding to the N−H stretching modes of proteins (not shown).

To visualize the small frequency shifts induced by the ^{15}N labeling on the amide I bands, the spectra previously shown in Figure 4 are presented in the spectral range 1730−1630 cm^{-1} (Figure 5). When the $P700^+/P700$ FTIR spectrum of the unlabeled and uniformly ^{15}N-labeled samples was compared, two main effects were detected. First, a small shift (<1 cm^{-1}) of the large differential signal at 1698 (−)/1688-(+) cm^{-1} in the $P700^+/P700$ FTIR spectrum of the unlabeled samples gives rise to a band centered at 1691 cm^{-1} in the double-difference spectrum (Figure 5c). Second, a relatively larger perturbation is observed for the differential signal at 1651(+)/1642(−) cm^{-1} in the spectrum of the unlabeled sample, which downshifts by 1−2 cm^{-1} upon ^{15}N labeling. The latter effect, which gives rise to the 1654/1648 cm^{-1} differential signal in the double-difference spectrum (lower trace of Figure 5), is more characteristic of a protein amide I mode than a 9-keto Chl C═O mode (*22*).

DISCUSSION

Comparison with the $P700^+/P700$ FTIR Spectra of Other Mutants at Thr PsaA739. Although the present $P700^+/P700$ FTIR spectroscopic study is the first report of mutants at the Thr A739 site in the cyanobacterium *Synechocystis*, two previous studies have reported FTIR spectra of mutants at the same site in the algae *C. reinhardtii*. Notably, this key

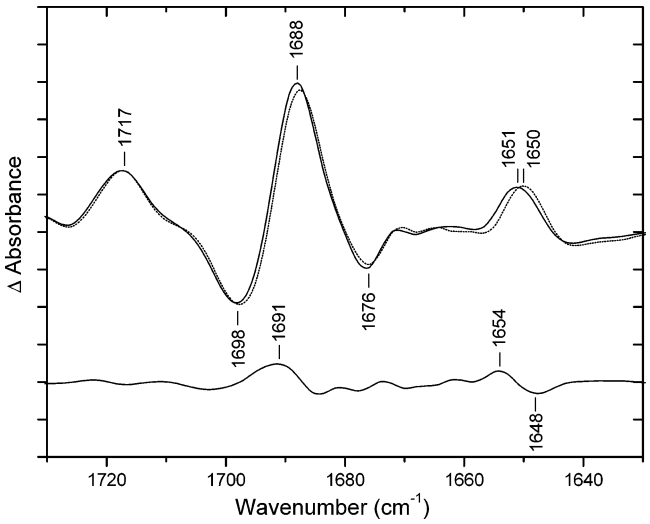

FIGURE 5: Expended view of the spectra of PS I complexes from the triple mutant shown in Figure 4. The traces for unlabeled (—) and ^{15}N-labeled (•••) PS I are overlaid in the top part of the figure. The double-difference spectrum of the unlabeled minus ^{15}N-labeled is shown as the bottom trace.

Thr residue has been replaced with Tyr, His, and Val (*17*) and by Ala (*18*). In all cases, the reported P700$^+$/P700 FTIR spectra show a strong reduction of the amplitude of the differential signal centered around 1645 cm^{-1} in the wild type together with the appearance of a new differential signal centered at higher frequency in the spectrum of the mutants. This is closely comparable to what is observed in the present study, where the 1653(+)/1638(−) cm^{-1} differential signal in the spectrum of the wild type is replaced by a differential signal negative at 1676 cm^{-1} and positive at 1688 cm^{-1} after mutation (Figures 2 and 3).[2]

In the study by Witt et al. (*17*), it was further observed that the frequency of the new negative band appearing in the spectra of the mutants was dependent upon the nature of the residue introduced at the mutated site, suggesting that it was determined by the possibility of the new residue to engage in hydrogen-bonding interactions with the 9-keto carbonyl of P_A. This negative band was found at 1657, 1669, or 1672 cm^{-1} upon replacing Thr by Tyr, His, or Val, respectively. The latter frequency was also observed for the negative band in the study by Wang et al. (*18*), where Ala was introduced at the same position.

Shifts and amplitude changes of the C═O ester bands of the Chls of P700 observed above 1725 cm^{-1} have been described upon T(A739)A mutation, leading to band assignments (*18*). While the assignments of the two differential signals found at higher frequency are the same as those previously proposed on the basis of the comparison of the P700$^+$/P700 and ^{3}P700/P700 FTIR spectra (*9*), the small signal around 1730 cm^{-1} was assigned to the 7c-ester C═O of P_A. It should be noticed that the perturbation of these C═O ester bands described for the Thr to Ala mutation in *C. reinhardtii* (*18*) has no counterparts in the case of the T(A739)F single mutant in *Synechocystis*, investigated here as only a ∼1 cm^{-1} upshift of the small differential signal at 1735(−)/1730(+) cm^{-1}, observed upon mutation (parts a and b of Figure 2). Further studies will be required to find out whether this difference is primarily due to the different species involved or is related to the nature of the residue introduced at the Thr A739 site.

Effect of Mutations at Thr A739 on the 9-Keto C═O Vibration of the PsaA Chl of P700. Upon combining global isotope labeling and a comparison of P700$^+$/P700 and ^{3}P700/P700 FTIR difference spectra, the 9-keto and 10a-ester C═O modes of the two Chls in P700 and P700$^+$ were assigned (*9*). When these assignments could be correlated with the high-resolution structure of PS I (*10*), it became possible to identify the 9-keto and 10a-ester C═O modes of P_A, P_A^+, P_B, and P_B^+ (*6*). Notably, a differential signal at 1656(+)/1637(−) cm^{-1} in the P700$^+$/P700 spectrum of wild-type *Synechocystis* at 90 K was assigned to the upshift upon photooxidation of the 9-keto mode of P_A in strong hydrogen-bonding interaction with the OH group of Thr A739 (*6*, *9*).

Therefore, the upshift by ∼30−40 cm^{-1} of the 1657−1660(+)/1637(−) cm^{-1} differential signal observed for both the single T(A739)F mutant and the triple mutant (Figures 2c and 3c) when the Thr residue in hydrogen-bonding interaction with the 9-keto C═O group of P_A is perturbed fits well within our previously proposed assignment scheme (*6*, *9*). The same model has been used to rationalize the effect of the mutations at Thr A739 in *C. reinhardtii* although the possibility that the observed spectral changes around 1630−1660 cm^{-1} could be obscured by absorption changes of the amide I protein band was not considered (*17*). On the other hand, a very different assignment scheme has been used to explain the equivalent changes observed when the Thr residue was mutated to Ala (*18*). This point will be discussed in a subsequent section.

It is worth noting that only a fraction of the differential signal centered around 1645 cm^{-1} upshifts upon T(A739) mutations (Figures 2 and 3), leaving a differential signal at 1651(+)/1642(−) cm^{-1}. A comparable feature is also present in the T(A739)A mutant in *C. reinhardtii* (*18*). These remaining signals could have different origins. It could represent a side-chain contribution or the amide I signature of a protein conformational and/or electrostatic change. Alternatively, it could also correspond to the upshift upon P700 photooxidation of the 9-keto C═O carbonyl group of a fraction of P_A that would remain in hydrogen-bonding interaction with the OH group of a water molecule present in the mutated cavity (or with the OH side chain of the Tyr introduced at the PsaA 739 site in the triple mutant). To test between these possibilities, global ^{15}N labeling of the triple mutant was used. For isolated Chl *a* it has been demonstrated that the 9-keto C═O vibration was essentially insensitive to the labeling of the centrally located nitrogen atoms (*9*). On the other hand, the coupling between the C═O and N−H modes within the peptide bond leads to a small downshift (1−3 cm^{-1}) of the amide I mode upon ^{15}N labeling (*22*). Therefore, the ∼1−2 cm^{-1} downshift upon global ^{15}N labeling of the 1651(+)/1642(−) cm^{-1} differential signal in the P700$^+$/P700 FTIR spectrum of the triple mutant (Figure 5) preferentially indicates a protein conformational change rather than a contribution from the 9-keto C═O group of a

[2] The positive band at 1651 cm^{-1} that remains in the P700$^+$/P700 FTIR spectra of the mutants (Figures 2b and 3b) appears to contribute significantly to the band at 1653 cm^{-1} in the P700$^+$/P700 FTIR spectrum of the wild-type (Figure 2a). Such a contribution explains that the positive band in the wild type minus mutant double-difference spectra is apparently shifted to 1657−1660 cm^{-1} (Figures 2c and 3c).

subpopulation of P_A.[3] This conclusion reinforces our earlier observation (*16*) that it was somewhat hazardous to assign the differential signal centered around 1645 cm^{-1} in the $P700^+/P700$ FTIR spectrum of the wild type to the 9-keto C=O of P_A solely on the basis of the effect of mutations (*17*). It is interesting to note that global ^{15}N labeling also elicits a small effect on the large $P700^+/P700$ bands located around 1680−1690 cm^{-1} (Figure 4). Comparable effects have been detected previously for the wild type (*9*). It is therefore likely that the positive band at 1688 cm^{-1} in $P700^+/P700$ FTIR spectra of both the mutants and the wild type contains some contributions from protein amide I modes. This proposal appears highly probable in view of the existence of a sizable contribution from amide II modes (Figure 4). Additional contributions from protein modes that are sensitive to photooxidation of P700 and that differ between wild type and mutants are probably responsible for some of the differences seen around 1660−1670 cm^{-1} in the $P700^+/P700$ FTIR difference spectra of both the wild type and the mutants (Figures 2 and 3).

When the $P700^+/P700$ FTIR spectra of the single T(A739)F mutant (Figure 2b) and the triple mutant (Figure 3b) are compared, the bands assigned to the P_A^+/P_A vibrations of the 9-keto C=O group are found at identical frequencies at 1688/1676 cm^{-1} in both mutants. Similarly, when the hydrogen-bonding Thr residue A739 in *C. reinhardtii* is replaced by the non-hydrogen-bonding residues Val (*17*) or Ala (*18*), the P_A^+/P_A 9-keto C=O vibrations are observed at 1688/1672 cm^{-1}. The corresponding frequencies for the bands assigned to P_B^+/P_B 9-keto C=O vibrations are 1718/1698 cm^{-1}. For the 9-keto C=O group of Chl a^+/Chl *a* in tetrahydrofuran, the corresponding values are 1718/1693 cm^{-1} (*11*). The ∼20−30 cm^{-1} frequency downshift observed for the P_A^+/P_A 9-keto C=O vibrations in the mutants compared to P_B^+/P_B or Chl a^+/Chl *a* in solution suggests that the 9-keto C=O group of P_A and P_A^+ is in hydrogen-bonding interaction with a water molecule in the T(A739)F mutant of *Synechocystis* and the T(A739)V and T(A739)A mutants of *C. reinhardtii*. In the case of the triple mutant of *Synechocystis*, it is also possible that the hydrogen-bond donor is the OH side chain of the introduced Tyr residue.

Finally, for the triple mutant, the observation that the mutations introduced at the two sites in addition to Thr A739 have no effect on the 9-keto C=O mode of P_A is consistent with the X-ray model that shows Thr A739 as the only residue in hydrogen-bonding interaction with the 9-keto C=O mode of P_A (*10*). Introducing other amino acid side chains at the Thr A739 site will be necessary to explore in more details the effect of the strength of hydrogen bonds and the polarity of the local environment on the IR frequency of the 9-keto C=O mode in P_A and P_A^+ and to compare it to the corresponding frequencies of 1698 and 1718 cm^{-1} for P_B and P_B^+, respectively.

Effect of the Triple Mutation on the 10a-Ester C=O Vibrations of the PsaA Chl of P700. The observation that neither the single T(A739)F mutation nor the triple mutation perturbs the 1754(+)/1749(−) cm^{-1} differential signal present in the spectrum of the wild type (Figure 2b) provides further support to our previous assignment of this band to the 10a-ester C=O group of P_B that is free from hydrogen-bonding interaction (*6*, *9*). The T(A739)F mutation has very little impact on the $P700^+/P700$ FTIR absorption changes assigned to the C=O ester vibrations of the Chl of P700 (Figure 2). This is taken to indicate that the water molecule H_2O-19, which is held by several residues, including Thr A739, and is proposed to be the hydrogen-bond donor to the bridging oxygen of the 10a-carbomethoxy group of P_A, is probably still present in the single T(A739)F mutant. It is possible that the minute upshift upon the T(A739)F mutation of the small differential signal at 1735(−)/1730(+) cm^{-1} in the $P700^+/P700$ spectrum of the wild type (Figure 2) results from a minor displacement of H_2O-19. On the other hand, the spectrum of the triple mutant is significantly modified in this frequency range. Notably, a complex set of two negative bands at 1735 and 1726 cm^{-1} with a positive band located in between at 1730 cm^{-1} in the wild-type spectrum is strongly affected, while a new positive band appears at 1762 cm^{-1} in the triple mutant (Figure 3). These observations clearly show that a perturbed 10a-ester C=O group of P_A, absorbing at a frequency lower than that of an unbound Chl 10a-ester C=O group, becomes free of interaction when Tyr A599, Ser A603, and Thr A739 are simultaneously replaced by their PsaB homologues Leu, Gly, and Tyr, respectively. This suggests that in the triple mutant, the H_2O-19 water is either no longer present in the site or, at least, is interacting much less with the 10a-carbomethoxy group of P_A. Previously, a 1740(+)/1733(−) cm^{-1} differential signal in the $P700^+/P700$ FTIR difference spectrum of *Synechocystis* at 90 K was assigned to the upshift upon photooxidation of the 10a-ester C=O group of P_A (*6*, *9*). Recently, the same assignment scheme has also been favored in *C. reinhardtii* at ambient temperature (*18*). At first sight, the frequency upshift of a 10a-ester C=O group upon removal of the hydrogen bonds to water H_2O-19 observed in the present study also appears to support our previous assignment (*6*, *9*).

However, the precise assignment of the set of bands observed in the frequency range of 1725−1745 cm^{-1} still appears problematic. The first difficulty originates from the complex hydrogen-bond network involving H_2O-19 and the very peculiar nature and geometry of the hydrogen bond between this water molecule and the bridging oxygen of the 10a-carbomethoxy group of P_A (Figure 1). In the X-ray structural model of P700, the 10a-ester C=O group of P_A is free from hydrogen-bonding interaction, while the methoxy oxygen is hydrogen-bonded to the H_2O-19 water molecule (*10*). Therefore, in principle, hydrogen bonding to the methoxy oxygen is expected to decrease partial conjugation between the methoxy C−O and the ester C=O bonds, resulting in an upshift of the C=O frequency. However, this reasoning does not take into account the effect of the partial conjugation of the whole 10a-carbomethoxy group to ring V of the Chl macrocycle. The extent of this partial conjugation, which apparently can considerably lower the frequency of the 10a-ester C=O group, depends on the diedral angle between the O−C=O plane of the carbomethoxy group and that of ring V. This angle will be modulated by the presence of hydrogen bonds to the carbomethoxy oxygen atoms as

[3] However, it should be cautioned that the absence of a measurable coupling of the 9-keto C=O mode with vibrational modes involving the Chl nitrogen atoms has been checked only for Chl *a* in solution (*9*) and that a different type of coupling could occur when the Chl is in a strained conformation induced by the binding to the protein.

well as by the various van der Waals contacts with the nearby atoms. The comparison of the FTIR spectra of the single T(A739)F mutant (Figure 2b) and of the triple mutant (Figure 3b) shows that the two additional mutations, S(A603)G and Y(A599)L, primarily induce a decrease of amplitude of a positive band present at 1731 cm^{-1} in the spectrum of the single mutant and the appearance of a band at 1762 cm^{-1} in the spectrum of the triple mutant. Our previous assignment of the IR contribution of the 10a-ester C═O group of P_A (*6*, *9*), which was based on the simple frequency upshift of the 10a-ester C═O group of Chl *a* upon cation formation in a solvent, would have been more consistent with the disappearance or the perturbation of the wild-type 1742(+)/1735(−) cm^{-1} differential signal and the appearance of a differential signal at a higher frequency in the spectrum of the triple mutant. One possibility to explain the more complex behavior observed for Chl *a* in P700 would be to consider that the response of the 10a-carbomethoxy group of P_A to $P700^+$ formation is to change its extent of conjugation to ring V, e.g., by changing its orientation with respect to the plane of the Chl macrocycle, and that the interaction with water H_2O-19 modulates this conjugation.

Another difficulty arises from the observation of the small 1730(+)/1726(−) cm^{-1} differential signal in the $P700^+$/P700 FTIR difference spectrum of wild-type *Synechocystis*. This third set of bands in the region of absorption of the C═O ester vibrations, which is barely noticeable in the 90 K spectra (*9*), was first ascribed to an unspecified 10a-ester C═O vibration of P700 on the basis of selective isotope labeling (*23*). A similar feature of small amplitude at 1731(+)/1728(−) cm^{-1} was also observed in the room-temperature $P700^+$/P700 FTIR difference spectrum of *C. reinhardtii* at 2 cm^{-1} resolution (*15*) and was recently assigned to the 7c-ester C═O of the PsaA Chl of P700 (18). The absence of a significant perturbation of the $P700^+$/P700 FTIR spectrum in the frequency range of the Chl ester C═O vibrations in the mutant Y(A731)F (Tang, H., Xu, W., M. P., P. C., and J. B., unpublished results), where the hydrogen-bonding interaction with the 7c-ester C═O of P_A in the wild type (Figure 1) should be disrupted, shows that such an assignment cannot be made for the equivalent 1730(+)/1726(−) cm^{-1} differential signal in *Synechocystis*.

Effect of the Mutations on the Conformation of the Macrocycle of the P700 Chls. One interesting observation for the $P700^+$/P700 FTIR spectra of both the single T(A739)F and the triple mutants is the 2−3 cm^{-1} downshift of the macrocycle C═C marker mode of 5-coordinated Chl at 1608 cm^{-1} (*21*) compared to the wild type. Similar perturbations of these modes have also been noticed in the spectrum of the T(A739)A mutant in *C. reinhardtii* (*18*). The spectral features assigned to the coupled C−C, C−H, and C−N modes of the Chl macrocycle absorbing between 1400 and 1250 cm^{-1} are also strongly affected by the mutations at the Thr A739 site (Figures 2 and 3). This shows that mutations at Thr A739 have a large impact on the conformation of the Chl ring of P700. Much smaller perturbations of these modes are observed in the mutants on the His axial ligand to P_B (*16*). It is therefore probable that the strong hydrogen bond between Thr A739 and the 9-keto C═O group of P_A is responsible for a strain of the Chl macrocycle and that the weakening of this hydrogen bond releases the strain. However, it is noticeable that the conformational change of the macrocycle induced by the T(A739)F mutation has only very little impact on the geometry and hydrogen-bonding status of the 10a-ester C═O group of the Chls of P700.

Discussion of the Assignment Scheme of Hastings et al. The assignment scheme for the 9-keto and 10a-ester C═O carbonyls of P700 used in the present study has been originally developed on the basis of a comparison of the $P700^+$/P700 and ^{3}P700/P700 FTIR spectra that showed clearly that the 9-keto C═O group of one of the Chl of P700 in *Synechocystis* absorbs at 1637 cm^{-1} at 90 K (*9*). The major functional outcome from these FTIR studies was that after photooxidation, the positive charge was essentially delocalized over the two Chl molecules in $P700^+$ with a distribution ranging between 1:1 and 2:1 in favor of P_B^+. In addition, the triplet state in ^{3}P700 was found to be fully localized on P_A (*6*, *9*). Both of these conclusions were at variance with those derived from magnetic resonance studies of $P700^+$ and ^{3}P700 in the wild-type and mutant samples, which were interpreted to show that both the spin in $P700^+$ and the triplet character in ^{3}P700 were essentially localized on P_B (*1*). This large discrepancy between the interpretation of the results of FTIR and magnetic resonance experiments led Hastings et al. (*15*) to propose an alternative assignment of bands for the 9-keto C═O groups of the P700 Chls in the $P700^+$/P700 FTIR difference spectra of *C. reinhardtii*. The essential difference between the assignments proposed by Hastings et al. (*15*) and ours (*6*, *9*, *16*) deals with the frequency of the bands of the 9-keto C═O group of P_A in P700 and $P700^+$. In the neutral state, this C═O group is proposed to absorb at 1697 cm^{-1} (*15*) or at 1637 cm^{-1} (*6*, *9*), while in $P700^+$, it is found at 1687 cm^{-1} (*15*) or at 1656 cm^{-1} (*6*, *9*).

Thus, in the assignment scheme of Hastings et al. (*15*), the 9-keto C═O group of P_A absorbs at a high frequency (1697 cm^{-1}) characteristic of a carbonyl group in an apolar environment and with no hydrogen-bonding interactions. Moreover, the 9-keto C═O group of this Chl is proposed to downshift by 10 cm^{-1} upon $P700^+$ formation. Such a downshift upon cation formation of the frequency of a C═O group conjugated to the ring V of Chl would be unprecedented. The formation of the cation state of BChl (*24*) or Chl (*11*) in solution is always accompanied by an upshift of the frequency of the 9-keto and 10a-ester C═O vibrations. Similarly, P^+ formation in purple bacteria (*25*), green bacteria (*25*−*27*), and heliobacteria (*25*, *28*), as well as generation of $P680^+$ in PS II (*29*, *30*), is characterized by an upshift of the frequency of the 9-keto and 10a-ester C═O vibrations. Even in the assignment scheme of Hasting et al. (*15*), the vibrations of the 9-keto C═O group of P_B and of the 10a-ester of both P_A and P_B upshift upon $P700^+$ formation. To explain such an unusual behavior of the 9-keto C═O group of P_A, one would probably have to invoke the establishment of an unusually strong hydrogen bond to this group in $P700^+$.

In a more recent study, essentially the same assignment scheme was used to interpret the effect of replacing the Thr A739 residue in hydrogen-bonding interaction with the 9-keto C═O group of P_A by an Ala residue in *C. reinhardtii* (*18*). The impact of the T(A739)A mutation on the bands assigned by Wang et al. (*18*) to the 9-keto C═O vibration of P_A and P_A^+ is actually very modest since this vibrational mode is proposed to upshift upon mutation by only 4 cm^{-1} from 1695 to 1699 cm^{-1} in P_A and by 2 cm^{-1} from 1686 to 1688 cm^{-1}

Table 2: Approximate Frequencies (cm^{-1}) of the $P700^+/P700$ Bands Assigned to the 9-Keto C=O Carbonyls of P_A and P_B in the Wild Type and the Thr A739 Mutant by Wang et al. (*18*) and in this Paper

	Wang et al. (*18*)		This paper	
	wild type	T(A739)A	wild type	T(A739)F
P_A	1695	1699	1637	1676
P_A^+	1686	1688	1660	1689
P_B	1704	1704	1698	1698
P_B^+	1716	1713	1718	1717

in P_A^+ (*18*). A comparison with the corresponding assignments proposed in the present work for the wild type and the T(A739)F mutant in *Synechocystis* is given in Table 2. When the assignments in Wang et al. (*18*) are taken at face value, the straightforward interpretation of the 9-keto C=O frequencies proposed for P_A and P_A^+ by Wang et al. (*18*) would be to consider that this carbonyl group of P_A is free from bonding interactions in both the wild type and mutant and that an unusually strong hydrogen bond to the 9-keto C=O group is present in P_A^+ and is essentially unchanged upon mutation. Such assignments are difficult to reconcile with the presence of the hydrogen bond to the 9-keto C=O group of P_A in the structural model of P700 (10). The data in Table 2 can be compared to the other example of the effect of mutations affecting the hydrogen bonding of the 9-keto C=O groups of the primary electron donor on the P^+/P FTIR difference spectra. When the non-hydrogen-bonding Leu residues M160 and L131 located near the 9-keto C=O groups of P in *Rhodobacter sphaeroides* are replaced by His side chains, the frequency downshift for the bands assigned to the 9-keto C=O groups in the P_L^+/P_L and P_M^+/P_M transitions were found to vary in the range of 20−35 cm^{-1} (*31*). The latter range of values for the mutation-induced frequency shifts is much closer to the 30−40 cm^{-1} range corresponding to the assignment scheme reported in the present study (Table 2) than to the 2−4 cm^{-1} range proposed by Wang et al. (*18*). The effect of the T(A739)A mutation in *C. reinhardtii* on the 9-keto C=O vibration of P_B and P_B^+ and on the 10a-ester C=O modes is either absent or very minor, and the corresponding bands keep the same assignments as proposed previously (*6*, *9*, *16*).[4]

The wild-type minus T(A739)F mutant double-difference spectrum in *Synechocystis* is dominated by two differential signals of opposite signs at 1660(+)/1637(−) cm^{-1} and 1689(−)/1676(+) cm^{-1} (Figure 2c), which have been assigned in the present work to the 9-keto C=O vibrations of P_A^+/P_A in the wild type and mutant. A set of two closely comparable features at 1660(+)/1636(−) cm^{-1} and 1690(−)/1672(+) cm^{-1} also dominates the equivalent double-difference spectrum for the T(A739)A mutation in *C. reinhardtii* (*18*), and therefore the assignment should be the same for these comparable mutations in the two species. Rather, in the assignment scheme of Hastings et al. (*15*, *18*), the differential signal at 1654(+)/1637(−) cm^{-1} in the $P700^+/P700$ FTIR difference spectrum of the wild type is proposed to arise from the imidazole C_4=C_5 mode from the His axial ligands to the Mg atom of the P700 Chls. The frequency of 1637 cm^{-1} for a C_4=C_5 imidazole mode coordinated to the Mg atom at N_τ and protonated at N_δ (*16*) is difficult to reconcile with the usual frequency range of 1606−1593 cm^{-1} established for this mode in 4-methylimidazole (*32*). Furthermore, the $P700^+/P700$ FTIR difference spectrum of *Synechocystis* isotope-edited with uniformly ^{13}C-labeled His has revealed a small band at 1612 cm^{-1} with an amplitude and a position adequate to be identified with the C_4=C_5 mode from the His axial ligands of P700 (*16*, *32*). Therefore, the proposed assignment of the differential signal at 1654(+)/1637(−) cm^{-1} to an imidazole C_4=C_5 mode (*15*, *18*) is incompatible with the present observations. Relevant to this point, in a very recent publication from the group of Hastings (*33*), the authors have dismissed their previous assignment. It is of note, however, that they do not provide an alternative assignment for the large differential signal at 1654(+)/1637(−) cm^{-1} in their $P700^+/P700$ FTIR difference spectrum of the wild-type *C. reinhardtii*.

Implications of the FTIR Results for Charge Distribution in $P700^+$. The distribution of the positive charge over the two Chls of $P700^+$ is an important parameter related to the $P700^+/P700$ midpoint redox potential, to the charge transfer properties, and possibly, to the directionality of PS I electron transfer reactions. Besides FTIR difference spectroscopy, ENDOR is the most prominent technique that has been extensively used to address the question of the electronic structure of $P700^+$ (*1*, *34*, *35*). From the most detailed studies (*1*), it has been concluded that P_B carries all or most of the spin density in $P700^+$, while P_A carries no or little (0−15%) spin density. Possible explanations for the stringent discrepancy between the rather symmetrical charge distribution in $P700^+$ derived from FTIR spectroscopy and the highly anisotropic distribution of spin density determined by ENDOR have been discussed previously (*16*). Notably, it was stressed that the conclusion from ENDOR is based essentially on the comparison of the sum of the assigned proton hfc's of three methyl groups of P_B^+ with those in isolated Chl a^+ (*12*), although the authors of the magnetic resonance studies have provided various reasons why such a comparison could be unreliable in the case of $P700^+$ (*1*, *12*, *17*). It has been further proposed that the small amount of electron spin density located on the three assigned methyl groups of P_B^+, which are not conjugated to the Chl macrocycle, may not

[4] Wang et al. (*18*) use the minor frequency shifts observed for the effect of the mutation on the frequency of the bands that they assign to the C=O groups of P_A and P_B as a mean to quantify the redistribution of the positive charge among the two Chls in $P700^+$ without considering that the frequency of these bands could be affected by slight changes in the strength of the hydrogen-bonding interactions and/or the electrostatic environment of these groups between the wild type and mutants.

[5] The frequency shift of the Chl 9-keto vibrations upon cation formation for P700 in the wild type is +20−23 cm^{-1} for P_A and +20 cm^{-1} for P_B. These values compare well with that of +25 cm^{-1} for isolated Chl *a* in tetrahydrofuran (*11*), consistent with the view that the positive charge is essentially localized on either P_A or P_B on the subpicosecond time scale of the IR measurement. If the frequency shifts of the 9-keto and 10a-ester vibrations in the $P700^+/P700$ FTIR difference spectra were exclusively due to changes of bond order upon cation formation, analyzing their magnitude should provide a narrower range for the charge distribution between P_A^+ and P_B^+. However, a more quantitative analysis has not been attempted for lack of knowledge of the effect of possible changes in the strength of the hydrogen-bonding interactions to the 9-keto groups upon $P700^+$ formation as well as of possible contributions from electrochromic effects on the Chl half of P700 on which the charge is not localized. Such effects could explain why the apparent cation-induced upshift of the 9-keto of P_A is only +13−14 cm^{-1} in the mutants.

be directly related to the average distribution of the unpaired electron between P_A^+ and P_B^+ (*16*). More recently, semiempirical quantum chemical calculations have been taken to indicate that, owing to spin polarization effects, the spin asymmetry in $P700^+$ could be significantly larger than the charge asymmetry (*36*).

In the FTIR experiments, the charge density distribution between P_A^+ and P_B^+ has been qualitatively assessed by the relative amplitudes of the differential signals assigned primarily to the change of bond order of the 9-keto and 10a-ester C═O groups of the two Chls of P700 upon photooxidation (*6*, *9*). Upon assuming that the extinction coefficients for these groups were comparable for the P_A^+/P_A and P_B^+/P_B transitions, it was concluded that the charge density distribution between P_A^+ and P_B^+ was in the range from 1:1 to 2:1 in favor of P_B.[5] This conclusion of a rather symmetrical charge distribution in $P700^+$ has been further supported by an independent FTIR measurement of the relative perturbation of the imidazole $C_5-N\tau$ stretching mode of the His axial ligand of P_A and P_B (*16*).

In the present study of the Thr A739 mutants, the wild-type minus mutant double-difference spectra (Figures 2c and 3c and Table 2) show that the 30−40 cm^{-1} frequency upshift upon mutation of the differential signal assigned to the 9-keto C═O group of P_A^+/P_A affects only marginally the amplitude of this differential signal. The peak to peak amplitude of the P_A^+/P_A differential signal increases by ∼5 and ∼25% in the triple mutant and the T(A739)F single mutant, respectively. A comparable observation is also valid for the T(A739)A mutation in *C. reinhardtii* (*18*), provided our assignment scheme is used. In the spectra of all of these mutants, a small decrease by 15−20% of the peak to peak amplitude of the differential signal assigned to the 9-keto C═O group of P_B^+/P_B can be noticed relative to the spectrum of the wild type. This may indicate a slight redistribution of the positive charge toward P_A^+ upon Thr A739 mutation. It should also be pointed out that, even after this small mutation-induced redistribution of charge has occurred, the amplitude of the P_A^+/P_A differential signal remains close to or somewhat smaller than that of the P_B^+/P_B differential signal. Hence, it can be concluded that the strong hydrogen bond to the 9-keto C═O group of P_A modulates only marginally the distribution of the charge in $P700^+$.

In conclusion, the effect of mutations at the Thr A739 site on the $P700^+$/P700 FTIR difference spectra in *Synechocystis* reported here is consistent with the band assignment scheme previously used to interpret the spectra (*6*, *9*, *16*). This observation is strengthened by the results of previous FTIR studies of other mutants at the same site in *C. reinhardtii* by Witt et al. (*17*) and Wang et al. (*18*), although in the latter case, a very different assignment scheme was used. Therefore, the results derived from the present FTIR study reinforce the view of a strong delocalization of the positive charge over the two Chl molecules in $P700^+$.

ACKNOWLEDGMENT

The authors thanks G. Ajlani, E. Nabedryk, W. Leibl, H. Tang, and W. Xu for stimulating discussions.

REFERENCES

1. Weber, A. N., and Lubitz, W. (2001) P700: The primary electron donor of photosystem I, *Biochim. Biophys. Acta 1507*, 61−79.
2. Hoff, A. J., and Deisenhofer, J. (1997) Photophysics of photosynthesis: Structure and spectroscopy of reaction centers of photosynthetic bacteria, *Phys. Rep. 287*, 1−247.
3. Mäntele, W. (1993) Infrared vibrational spectroscopy of the photosynthetic reaction center, in *The Photosynthetic Reaction Center* (Deisenhofer, J., and Norris, J. R., Eds.) Vol. 2, pp 239−283, Academic Press, San Diego, CA.
4. Nabedryk, E. (1996) Light-induced Fourier transform infrared difference spectroscopy of the primary electron donor in photosynthetic reaction centers, in *Infrared Spectroscopy of Biomolecules* (Mantsch, H. H., and Chapman, D., Eds.) pp 39−81, Willey-Liss, New York.
5. Breton, J., and Nabedryk, E. (1996) Protein-quinone interactions in the bacterial photosynthetic reaction center: Light-induced FTIR difference spectroscopy of the quinone vibrations, *Biochim. Biophys. Acta 1275*, 84−90.
6. Breton, J. (2001) Fourier transform infrared spectroscopy of primary electron donors in type I photosynthetic reaction centers, *Biochim. Biophys. Acta 1507*, 180−193.
7. Krauss, N., Schubert, W.-D., Klukas, O. P., Fromme, P., Witt, H. T., and Saenger, W. (1996) Photosystem I at 4 Å resolution represents the first structural model of a joint photosynthetic reaction centre and core antenna system, *Nat. Struct. Biol. 3*, 965−973.
8. Redding, K., MacMillan, F., Leibl, W., Brettel, K., Hanley, J., Rutherford, A. W., Breton, J., and Rochaix, J.-D. (1998) A systematic survey of conserved histidines in the core subunits of photosystem I by site-directed mutagenesis reveals the likely axial ligands of P_{700}, *EMBO J. 17*, 50−60.
9. Breton, J., Nabedryk, E., and Leibl, W. (1999) FTIR study of the primary electron donor of photosystem I (P700) revealing delocalization of the charge in $P700^+$ and localization of the triplet character in ^{3}P700, *Biochemistry 38*, 11585−11592.
10. Jordan, P., Fromme, P., Witt, H. T., Klukas, O., Saenger, W., and Krauss, N. (2001) Three-dimensional structure of cyanobacterial photosystem I at 2.5 Å resolution, *Nature 411*, 909−917.
11. Nabedryk, E., Leonhard, M., Mäntele, W., and Breton, J. (1990) Fourier transform infrared difference spectroscopy shows no evidence for an enolization of chlorophyll *a* upon cation formation either in vitro or during P700 photooxidation, *Biochemistry 29*, 3242−3247.
12. Käss, H., Fromme, P., Witt, H. T., and Lubitz, W. (2001) Orientation and electronic structure of the primary donor radical cation $P_{700}^{+\bullet}$ in photosystem I: A single-crystal EPR and ENDOR study, *J. Phys. Chem. B 105*, 1225−1239.
13. Krabben, L., Schlodder, E., Jordan, R., Carbonera, D., Giacometti, G., Lee, H., Weber, A. N., and Lubitz, W. (2000) Influence of the axial ligands on the spectral properties of P700 of photosystem I: A study of site-directed mutants, *Biochemistry 39*, 13012−13025.
14. Witt, H., Schlodder, E., Teutloff, C., Bordignon, E., Carbonera, D., Niklas, J., and Lubitz, W. (2001) Site-directed mutagenesis of Thr A739 of photosystem I in *Chlamydomonas reinhardtii* alters significantly the excitonic and electronic coupling of the primary electron donor P700, in *PS2001 Proceedings of the 12th International Congress of Photosynthesis*, S6−011, CSIRSO Publishing, Collingwood, Victoria, Australia.
15. Hastings, G., Ramesh, V. M., Wang, R., Sivakumar, V., and Weber, A. (2001) Primary donor photooxidation in photosystem I: A re-evaluation of ($P700^+$−P700) Fourier transform infrared difference spectra, *Biochemistry 40*, 12943−12949.
16. Breton, J., Xu, W., Diner, B. A., and Chitnis, P. (2002) The two histidine axial ligands of the primary electron donor chlorophylls (P700) in photosystem I are similarly perturbed upon $P700^+$ formation, *Biochemistry 41*, 11200−11210.
17. Witt, H., Schlodder, E., Teutloff, C., Niklas, J., Bordignon, E., Carbonera, D., Kohler, S., Labahn, A., and Lubitz, W. (2002) Hydrogen bonding to P700: Site-directed mutagenesis of threonine A739 of photosystem I in *Chlamydomonas reinhardtii*, *Biochemistry 41*, 8557−8569.
18. Wang, R., Sivakumar, V., Li, Y., Redding, K., and Hastings, G. (2003) Mutation induced modulation of hydrogen bonding to P700 studied using FTIR difference spectroscopy, *Biochemistry 42*, 9889−9897.
19. Xu, W., Chitnis, P., Valieva, A., van der Est, A., Pushkar, Y. N., Krzystyniak, B., Teutloff, C., Zech, S. G., Bittl, R., Stehlik, D., Zybailov, B., Shen, G., and Golbeck, J. H. (2003) Electron transfer in cyanobacterial Photosystem I. I. Physiological and spectroscopic characterization of site-directed mutants in a putative electron-

transfer pathway from A_0 through A_1 to F_X, *J. Biol. Chem. 278*, 27864−27875.
20. Sun, J., Ke, A., Jin, P., Chitnis, V. P., and Chitnis, P. R. (1998) Isolation and functional studies of Photosystem I subunits in the cyanobacterium *Synechocystis* sp. PCC 6803, *Methods Enzymol. 297*, 124−139.
21. Fujiwara, M., and Tasumi, M. (1986) Metal-sensitive bands in the Raman and infrared spectra of intact and metal-substituted chlorophyll *a*, *J. Phys. Chem. 90*, 5646−5650.
22. Noguchi, T., and Sugiura, M. (2003) Analysis of flash-induced FTIR difference spectra of the S-state cycle in the photosynthetic water-oxidizing complex by uniform ^{15}N and ^{13}C isotope labeling, *Biochemistry 42*, 6035−6042.
23. Kim, S., and Barry, B. A. (2000) Identification of carbonyl modes of P700 by in situ chlorophyll labeling in photosystem I, *J. Am. Chem. Soc. 122*, 4980−4981.
24. Mäntele, W., Wollenweber, A. M., Nabedryk, E., and Breton, J. (1988) Infrared spectroelectrochemistry of bacteriochlorophylls and bacteriopheophytins: Implications for the binding of the pigments in the reaction center from photosynthetic bacteria, *Proc. Natl. Acad. Sci. U.S.A. 85*, 8468−8472.
25. Nabedryk, E., Leibl, W., and Breton, J. (1996) FTIR spectroscopy of primary donor photooxidation in photosystem I, *Heliobacillus mobilis*, and *Chlorobium limicola*. Comparison with purple bacteria, *Photosynth. Res. 48*, 301−308.
26. Noguchi, T., Kusumoto, N., Inoue, Y., and Sakurai, H. (1996). Electronic and vibrational structure of the radical cation of P_{840} in the putative reaction center from *Chlorobium tepidum* as studied by FTIR spectroscopy, *Biochemistry 35*, 15428−15435.
27. Mezzetti, A., Seo, D., Leibl, W., Sakurai, H., and Breton, J. (2003) Time-resolved step-scan FTIR investigation of the reaction center from the green sulfur bacterium *Chlorobium tepidum*, *Photosynth. Res. 75*, 161−169.
28. Noguchi, T., Fukami, Y., Oh-oka, H., and Inoue, Y. (1997) Fourier transform infrared study on the primary donor P798 of *Heliobacterium modesticaldum*: Cysteine S−H coupled to P798 and molecular interactions of carbonyl groups, *Biochemistry 36*, 12329−12336.
29. Breton, J., Hienerwadel, R., and Nabedryk, E. (1997) FTIR difference spectrum of the photooxidation of the primary electron donor of photosystem II, in *Spectroscopy of Biological Molecules: Modern Trends* (Carmona, P., Navarro, R., and Hernanz, A., Eds.) pp 101−102, Kluwer, Dordrecht, The Netherlands.
30. Noguchi, T., Tomo, T., and Inoue, Y. (1998) Fourier transform infrared study of the cation radical of P_{680} in the photosystem II reaction center: Evidence for charge delocalisation on the chlorophyll dimer, *Biochemistry 37*, 13614−13625.
31. Nabedryk, E., Allen, J. P., Taguchi, A. K. W., Williams, J. C., Woodbury, N. W., and Breton, J. (1993). Fourier transform infrared study of the primary electron donor in chromatophores of *Rhodobacter sphaeroides* with reaction centers genetically modified at residues M160 and L131, *Biochemistry 32*, 13879−13885.
32. Hasegawa, K., Ono, T., and Noguchi, T. (2002) Ab initio density functional theory calculations and vibrational analysis of zinc-bound 4-methylimidazole as a model of a histidine ligand in metalloenzymes, *J. Phys. Chem. A 106*, 3377−3390.
33. Wang, R., Sivakumar, V., Johnson, T. W., and Hastings, G. (2004) FTIR difference spectroscopy in combination with isotope labeling for identification of the carbonyl modes of P700 in photosystem I, *Biophys. J. 86*, 1061−1073.
34. Deligiannakis, Y., and Rutherford, A. W. (2001) Electron spin−echo envelope modulation spectroscopy in photosystem I, *Biochim. Biophys. Acta 1507*, 226−246.
35. Rigby, S. E. J., Evans, M. C. W., and Heathcote, P. (2001) Electron nuclear double resonance (ENDOR) spectroscopy of radicals in photosystem I and related Type 1 photosynthetic reaction centres, *Biochim. Biophys. Acta 1507*, 247−259.
36. Plato, M., Krauss, N., Fromme, P., and Lubitz, W. (2003) Molecular orbital studies of the primary electron donor P700 of photosystem I based on a recent X-ray single-crystal analysis, *Chem. Phys. 294*, 483−499.

BI049515J